

Multi-Manifold Learning for Large-Scale Targeted Advertising System

Kyuyong Shin

ky.shin@navercorp.com

Clova AI Research, NAVER Corp.

Kyung-Min Kim

kyungmin.kim.ml@navercorp.com

Clova AI Research, NAVER Corp.

Young-Jin Park

young.j.park@navercorp.com

Naver R&D Center, NAVER Corp.

Sunyoung Kwon

sunny.kwon@navercorp.com

Clova AI Research, NAVER Corp.

ABSTRACT

Messenger advertisements (ads) give direct and personal user experience yielding high conversion rates and sales. However, people are skeptical about ads and sometimes perceive them as spam, which eventually leads to a decrease in user satisfaction. Targeted advertising, which serves ads to individuals who may exhibit interest in a particular advertising message, is strongly required. The key to the success of precise user targeting lies in learning the accurate user and ad representation in the embedding space. Most of the previous studies have limited the representation learning in the Euclidean space, but recent studies have suggested hyperbolic manifold learning for the distinct projection of complex network properties emerging from real-world datasets such as social networks, recommender systems, and advertising. We propose a framework that can effectively learn the hierarchical structure in users and ads on the hyperbolic space, and extend to the *Multi-Manifold Learning*. Our method constructs multiple hyperbolic manifolds with learnable curvatures and maps the representation of user and ad to each manifold. The origin of each manifold is set as the centroid of each user cluster. The user preference for each ad is estimated using the distance between two entities in the hyperbolic space, and the final prediction is determined by aggregating the values calculated from the learned multiple manifolds. We evaluate our method on public benchmark datasets and a large-scale commercial messenger system LINE, and demonstrate its effectiveness through improved performance.

KEYWORDS

Targeted Advertising, Messenger Advertising, Multi-Manifold Learning, Hyperbolic Space

ACM Reference Format:

Kyuyong Shin, Young-Jin Park, Kyung-Min Kim, and Sunyoung Kwon. 2020. Multi-Manifold Learning for Large-Scale Targeted Advertising System. In *AdKDD'20, August 23, 2020, San Diego, CA, USA*. ACM, New York, NY, USA, 6 pages. <https://doi.org/10.1145/1122445.1122456>

Permission to make digital or hard copies of all or part of this work for personal or classroom use is granted without fee provided that copies are not made or distributed for profit or commercial advantage and that copies bear this notice and the full citation on the first page. Copyrights for components of this work owned by others than ACM must be honored. Abstracting with credit is permitted. To copy otherwise, or republish, to post on servers or to redistribute to lists, requires prior specific permission and/or a fee. Request permissions from permissions@acm.org.

AdKDD'20, August 23, 2020, San Diego, CA, USA

© 2020 Association for Computing Machinery.

ACM ISBN 978-1-4503-XXXX-X/18/06...\$15.00

<https://doi.org/10.1145/1122445.1122456>



Figure 1: LINE messenger advertisement system.

1 INTRODUCTION

Messenger platform is an emerging advertisement channel. In messenger platform, users experience a message-typed advertisement (ad) with a separate chat room feeling more private and direct compared to traditional ad channels, e.g., search engine, and web portal. High penetration ratios of smartphone and SNS utilization enable messenger ad system to become more promising with high sales [26]. Figure 1 shows an example of our LINE messenger advertisement system.

However, an ad for broad random users without precise user targeting can not resonate with their potential audience playing as annoying spam. In this paper, since the accurate representation of the users and ads is a necessary for targeted advertising system, we present the deep representation learning scheme using hyperbolic geometries. Our method enables effective capture of the hierarchical and complex relationships between users and ads.

One of the most prominent approaches in traditional studies is Collaborative Filtering (CF) [4, 14, 24] which finds a group of users who have responded to the ads similar to the target ad. Owing to the limitation of the low-dimensional representation of CF, recent studies have presented neural network based approaches [4, 22, 23, 25] that can effectively embed user and advertisements into the high-dimensional spaces. Despite the wide success and expansion of those methodologies, most of them implicitly embed the entities

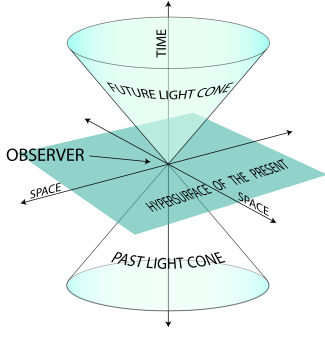


Figure 2: Minkowski space.

(i.e., users and ads) into points in Euclidean space, which causes an inherent limitation in the representation power. The latest studies, however, pointed out that the real-world user-item interaction datasets exhibits the hierarchical structures; therefore, it is more desirable to map embeddings into a hyperbolic space than Euclidean space [2, 15, 18, 21]. Unlike in the flat (Euclidean) plane, the distance between the nodes in tree-structured data is preserved in hyperboloid [9], and therefore hyperbolic geometry is proven to naturally suitable for modeling hierarchical structures.

Although the hyperbolic space has successfully reflected the topology in user-item representation, the existing approaches fix its origin and use single manifold as an embedding space. In a real-world, large-scale advertising system, there exist various groups of users with different preference characteristics, and it may not be valid to assume that every user and advertisement entity can be expressed by using single geometry. There were several researches in Euclidean space that improves the prediction performance by adopting clustering algorithms into the recommendation tasks [5, 8, 19]. However, usage of clustering scheme into the hyperbolic manifold learning on advertising system had not yet been reported. The main contribution of this paper is to extend the hyperbolic representation learning to the *Multi-Manifold Learning* framework by constructing multiple hyperbolic spaces centered on each clustered user group.

We evaluate the proposed framework on a large-scale real-world dataset collected from LINE messenger platform. The experimental results demonstrate that the proposed model increases the prediction performance and allows the representation to be diversified. We further report the performance on the public benchmark datasets to show that Multi-Manifold Learning can be applied commonly to various tasks as well as the targeted advertising.

2 TARGETED ADVERTISING SYSTEM

Unlike the traditional forms of advertising that expose ads to random users, the core of targeted advertising is that the system sends ads to different user groups based on the user-ad-preferences. The targeted advertising system uses the side information of those ads, such as images and advertising phrases, as well as the user's demographic information and click history to find the most relevant user group.

Starting from the X_u for users and X_a for advertisements with attribute matrices $X_u \in \mathbb{R}^{N_u \times F_u}$ and $X_a \in \mathbb{R}^{N_a \times F_a}$, the neural

networks $f_u : \mathbb{R}^{F_u} \rightarrow \mathbb{R}^H$ and $f_a : \mathbb{R}^{F_a} \rightarrow \mathbb{R}^H$ transforms the X_u and X_a to $Z_u \in \mathbb{R}^{N_u \times H}$ and $Z_a \in \mathbb{R}^{N_a \times H}$, where F_u , N_u , and H denotes the number of attributes of $u \in \{u, a\}$, and the number of hidden features, respectively. To build a more powerful user representations, we introduce additional neural networks $f_h : \mathbb{R}^{F_a} \rightarrow \mathbb{R}^H$ that embeds users' click history matrix C into $Z_h \in \mathbb{R}^{N_u \times H}$ where $c_{i,j}$ is one if there is positive interaction between the i -th user and j -th advertisement and is zero otherwise.

Finally, the preference scores, $P_{u,a}$, between the users and ads are computed through the distance or inner-product between embeddings of them:

$$P_{u,a} = \text{Decision}(\text{dist}(Z_u + Z_h, Z_a)), \quad (1)$$

where $\text{dist}(p, q)$ is the distance between two points p and q on the given manifold. User preference scores are sorted for each ad, and the top k users with the highest scores are selected as the targeted users for the ad. In this paper, we used Fermi-Dirac decoder [11, 12] for the decision function.

3 HYPERBOLIC GEOMETRY

3.1 Riemannian Manifolds

A topological space \mathcal{M} is a smooth manifold if \mathcal{M} satisfies following four conditions: *It is Hausdorff, It is second countable, \mathcal{M} contained a open sets which is homeomorphic to \mathbb{R}^n , and its transition maps are infinitely differentiable.* For $p \in \mathcal{M}$, we can define the tangent space $T_p\mathcal{M}$ which is the first order approximation of \mathcal{M} around point p .

A Riemannian manifold is (\mathcal{M}, g) , where \mathcal{M} is a differential manifold and g is Riemannian metric, which is a family of inner products on tangent spaces, $g_p : T_p\mathcal{M} \times T_p\mathcal{M} \rightarrow \mathbb{R}$ with smoothly varying p . Riemannian metric is used to measure distances by integrating the length between two points:

$$d_g(p, q) = \inf \int_0^1 \sqrt{g_{\gamma(t)}(\dot{\gamma}(t), \dot{\gamma}(t))} \quad (2)$$

where $\gamma(0) = p$, $\gamma(1) = q$, and $\gamma \in C^\infty([0, 1], \mathcal{M})$. A shortest path between two points p and q on curve γ is called a geodesic, and equivalent to a straight line in Euclidean space. From geodesic, we can define the projection by utilizing geodesic coordinates. This is called *exponential map* \exp_p at p , which projects a vector v of the tangent space $T_p\mathcal{M}$ at p to a point $\exp_p(v) \in \mathcal{M}$ on the manifold. In this map, γ is the unique geodesic satisfying $\gamma(0) := p \in \mathcal{M}$ with unit-norm $\dot{\gamma}(0) := v \in T_p\mathcal{M}$. Consequently, in very local area, exponential map is satisfying $\exp_p(v) := \gamma(1)$. The reverse map is called *logarithmic map* that maps $q \in \mathcal{M}$ back to the tangent space $T_p\mathcal{M}$ at p such that $\log_p(\exp_p(v)) = v$.

3.2 Hyperbolic Space

Hyperbolic space is a non-Euclidean space with a constant negative Gaussian curvature. Gaussian curvature is the product of the principal curvature, which is divided into a sphere, hyperbola, and flat depending on whether the value is constantly positive, negative, or zero. Hyperbolic space is often associated with Minkowski spacetime in special relativity. Minkowski model is a n -dimensional hyperbolic geometry in which points are represented on the future light cone of a two-sheeted hyperboloid of $(n + 1)$ -dimensional Minkowski space as shown in Figure 2.

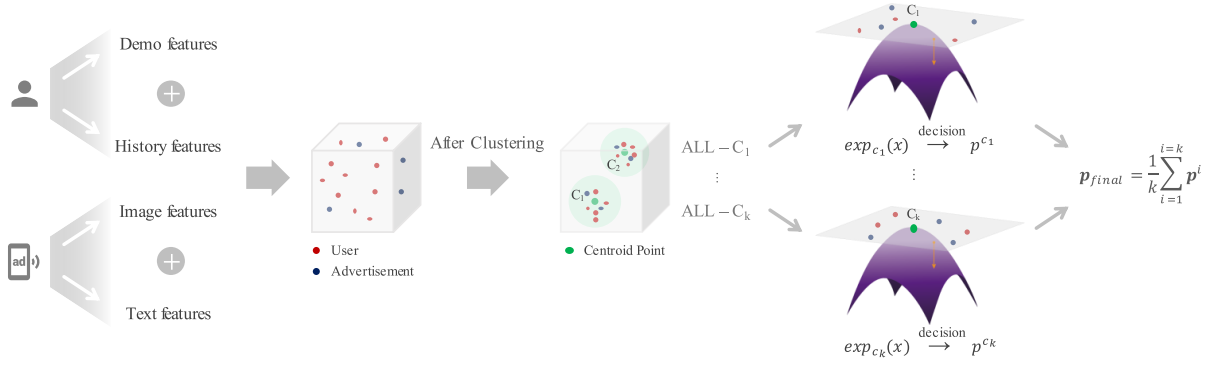


Figure 3: Conceptual scheme of our proposed method.

Table 1: Model Performance on LINE messenger advertisement system

	RocAuc	Accuracy	Average Precision	Shannon Entropy
CF	0.756	0.673	0.786	14.431
MLP	0.770	0.681	0.775	14.197
HNN	0.778	0.753	0.841	14.451
Multi-Manifold	0.818	0.765	0.846	14.567

Table 2: Model Performance on public benchmark MovieLens dataset

	MovieLens - 1M		MovieLens - 100K	
	RocAuc	Average Precision	RocAuc	Average Precision
CF	60.3	67.4	60.5	61.1
MLP	57.4	66.3	61.7	62.0
HNN	61.7	69.0	68.0	67.8
Multi-Manifold	61.5	69.8	68.3	68.5

The hyperbolic manifold is often considered as well-suited space for hierarchical structure. Suppose the task that embed a tree into the metric space while preserving its structural properties. i.e., the number of nodes at l -th layer is n^l . As a result, Euclidean space cannot contain all the nodes in the tree, which is linked to the poor representation of the model. However, in the hyperbolic space, the length of a circle is given as $2\pi\sinh r$ with the constant Gaussian curvature $K = -1$. Since $\sinh r = \frac{1}{2}(e^r - e^{-r})$, the circle length grow exponentially with r to enough to include all the nodes. This enables the learning of distinct representations of the data, which leads to the great potential of hyperbolic space for learning hierarchical relationships [3, 12].

Learning on hyperbolic manifold. Let $\langle \cdot, \cdot \rangle_{g_M}: \mathbb{R}^{n+1} \times \mathbb{R}^{n+1} \rightarrow \mathbb{R}$ denote the Minkowski inner product, $\langle p, q \rangle_{g_M} := -p_0q_0 + p_1q_1 + \dots + p_nq_n$ with the coordinates p_0 and q_0 representing time. We denote H^K as the hyperbolic manifold with constant negative curvature $-1/K$ ($K > 0$), and T_pH^K , the tangent space centered at point p . As described in Section 3.2, mapping between tangent space and manifold is performed by exponential and logarithmic maps. There are already known expressions of the exponential and the logarithmic maps on hyperboloid manifolds, which allow us to map points on hyperboloid to tangent spaces and vice-versa: For $p \in H^K$, $v \in T_pH^K$ and $q \in H^K$ such that $v \neq 0$ and $q \neq p$, the exponential and logarithmic maps of the hyperbolic model are given by:

$$\exp_p^K(v) = \cosh\left(\frac{\|v\|_{g_M}}{\sqrt{K}}\right)p + \sqrt{K}\sinh\left(\frac{\|v\|_{g_M}}{\sqrt{K}}\right)\frac{v}{\|v\|_{g_M}} \quad (3)$$

$$\log_p^K(q) = d_g^K(p, q) \frac{q + \frac{1}{K} \langle p, q \rangle_{g_M} p}{\|q + \frac{1}{K} \langle p, q \rangle_{g_M} p\|}, \quad (4)$$

where $\|v\|_{g_M} = \sqrt{\langle v, v \rangle_{g_M}}$ denotes norm of $v \in T_pH^K$ and $d_g^K(p, q) = \sqrt{K}\text{arccosh}(-\langle p, q \rangle_{g_M}/K)$ denotes geodesic distance between p and q . Above expressions assume that $\gamma_{p \rightarrow v}^K(t) = \cosh(\frac{t}{\sqrt{K}})p + \sqrt{K}\sinh(\frac{t}{\sqrt{K}})\frac{v}{\|v\|_{g_M}}$, when t is small enough and tangent vector v is unit-speed, i.e. $\langle v, v \rangle_{g_M} = 1$.

Diffeomorphism. The hyperbolic model tends to be more robust and stable than the Poincaré model, but the Poincaré model is easier to interpret and can visualize embeddings directly on the Poincaré disk. Fortunately, Poincaré disk is a stereographic projection of hyperboloid [6] which means these two models are homeomorphic and exists a diffeomorphism $\Psi(\cdot)$ mapping hyperbolic model onto the Poincaré model:

$$\Psi(x_0, x_1, \dots, x_d) = \frac{\sqrt{K}(x_1, x_2, \dots, x_d)}{x_0 + \sqrt{K}}, \quad (5)$$

we will utilize diffeomorphism $\Psi(\cdot)$ for visualizing embeddings of data in Figure 4.

4 MULTI-MANIFOLD LEARNING

The core functionality of our large-scale targeted advertising system is to capture the representational differences between various user groups and advertisements. To do this, we propose *Multi-Manifold Learning* that builds multiple manifolds for all user groups, and all manifolds are used for prediction as shown in Figure 3. Our proposed method consists of three stages. First, input X_u and X_a pass through DNNs f_u and f_a separately and users' click history C

Table 3: Model performance comparison as the number of cluster increases on LINE messenger dataset.

# of Clusters	RocAuc	Accuracy	Average Precision	Shannon Entropy
1-cluster	0.798	0.715	0.817	13.871
3-cluster	0.805	0.753	0.840	14.146
5-cluster	0.818	0.765	0.846	14.567
10-cluster	0.813	0.753	0.841	14.653
15-cluster	0.810	0.753	0.841	14.665

passes through transformer network [20] f_h . Second, calculate user embedding Z_{user} by adding Z_u and Z_h , and cluster them into T groups by using k -means clustering [1]. We denote c_t as a centroid of t -th group for $t \in \{1, \dots, T\}$. Finally, these embedding vectors map onto each t -th hyperbolic manifold of which the origin is c_t . Then, we calculate the preference score on each manifold using a Fermi-Dirac decoder [11, 12], and aggregate them.

The detailed process can be formulated as follow:

$$E_u^t = (Z_u + Z_h) - c_t, \quad E_a^t = Z_a - c_t \quad (6)$$

$$\exp_{\mathbf{o}}^K(E) = \left(\sqrt{K} \cosh\left(\frac{\|E\|_{Euc}}{\sqrt{K}}\right), \sqrt{K} \sinh\left(\frac{\|E\|_{Euc}}{\sqrt{K}}\right) \frac{E}{\|E\|_{Euc}} \right), \quad (7)$$

where E^t denotes embedding vector centered by centroid c_t . The $\exp_{\mathbf{o}}^K(E)$ represents Euclidean vector E mapped onto hyperbolic manifold with respect to the origin \mathbf{o} . It is essential to centering the Z with respect to centroid c_t of each user group. Optimizing often fails if manifold's origin is set to a point with a value other than the origin \mathbf{o} . The embeddings on each t -th hyperbolic manifold are used for computing user preference score through Fermi-Dirac decoder. Finally, our overall probability and loss are:

$$p_{u,a}^t = (1 + \exp^{(d_g^K(E_u^t, h, E_a^t, h) - s)/b})^{-1}, \quad E_h = \exp_{\mathbf{o}}^K(E) \quad (8)$$

$$\mathcal{L} = \sum \text{BCE}(P_{u,a}, Y), \quad (9)$$

where probability between user and ads on each manifold is $p_{u,a}^t$. And user preference of whole manifolds are $P_{u,a} = \frac{1}{T} \sum_{i=1}^T p_{u,a}^i$. The s and b in Fermi-Dirac decoder are hyper-parameter.

After mapping embeddings on the hyperboloid, an additional neural network layer such as Hyperbolic Neural Network (HNN) [7] can be added to perform weight learning on the hyperbolic manifold, but we empirically found that it does not show any performance improvements.

5 EXPERIMENT

5.1 Dataset

We collect dataset from LINE messenger platform that targets users from all over the world, and the number of users in the service is about 200 million. We randomly select one million users¹. We split a dataset based on time: the first fourteen days for training and the subsequent two days for test. We report the performance of the last epoch.

¹Since the number of users using the service is huge, we use a subset of users for experiments.

For better representation of user and advertisement embeddings, age, gender, mobile OS type, interest, number of LINE Pay membership follower, and number of LINE Pay membership followee attributes are used for users, while text and image are used for advertisements. For each attribute, we use shallow DNNs to make H -dimensional feature vectors and aggregate them to get the feature matrices Z_u and Z_a .

Due to a large number of users, we use 10,240 randomly sampled users for each batch. The advertisement click history is used up to the day before the forecast date, and click histories are normalized for each user.

For a fair comparison with the base models, we extend our experiments to public benchmark datasets: MovieLens², which is widely used public dataset for recommender systems. We modify the dataset to binary classification: a label as 1 if the movie score is greater than 4, otherwise as 0.

5.2 Baselines

To demonstrate the effectiveness of proposed model, we compared our model with following three base models:

- **Collaborative Filtering (CF)** [4, 14, 24]: The underlying assumption of Collaborative Filtering is the premise that users' past trends will remain the same in the future. In other words, it is a technique to identify users with similar patterns based on their preferences and interests.
- **Multilayer Perceptron (MLP)** [22, 23, 25]: There are numerous types of MLP algorithms that are based on Matrix Factorization. We report the presented framework using Euclidean space as MLP in the following results. Note that, Multi-Manifold Learning in Euclidean space is not reported, since the relative distance between two points is translation-invariant in Euclidean space.
- **Hyperbolic Neural Network (HNN)** [7]: This work generalizes the linear transform and bias addition of DNNs on the hyperbolic space and proposes several important deep learning tools on the hyperbolic space. We use HNN, which is based on basic DNNs, where the core operations are executed in hyperbolic space.

For the fairness of the comparison, we adopt the same neural network architectures for f_u and f_a . The hidden vector size is set to 64 and we do not use dropout [16] and l2 regularization. All the experiments were performed on NAVER SMART Machine Learning platform (NSML) [10, 17] using PyTorch [13].

5.3 Experimental Results and Analysis

We report three accuracy metrics of RocAuc, Accuracy, and Average Precision, and one diversity metric of Shannon Entropy. In particular, Average Precision is set up for the targeted Advertising System. The user preference is sorted for a specific advertisement, and then precision is calculated for each ad of the top k users. Finally, we average the precision of all ads.

Performance comparison. As shown in Table 1, our method shows the best prediction performance for all accuracy metrics, as well as the diversity metric. The diversity metric of Shannon entropy for each model shows how diversified the recommended users are. Our model shows the highest diversity compared to other

²<https://grouplens.org/datasets/movielens>

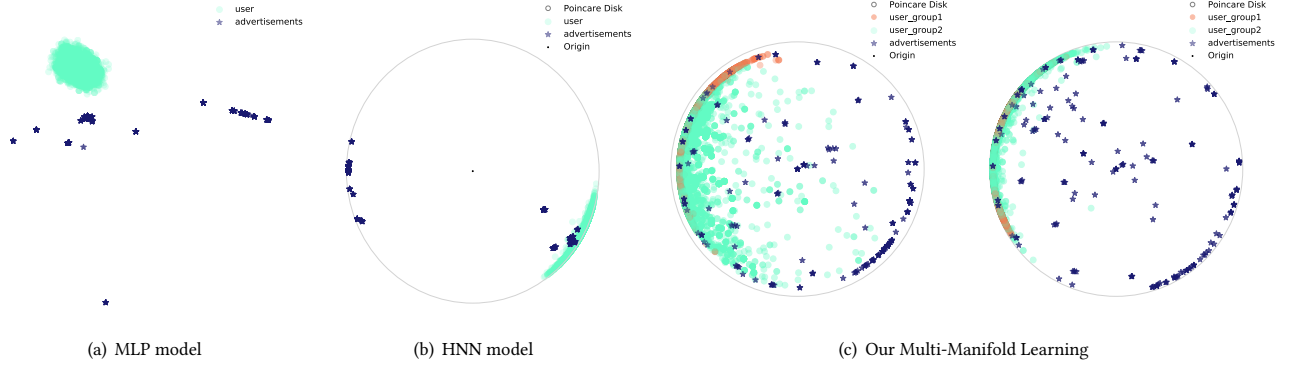


Figure 4: Visualization in embedding representations of users and advertisements. (a) embedding of Euclidean MLP, (b) Poincaré disk visualization of HNN, (c) Poincaré disk visualization of our Multi-Manifold Learning with two clusters on each manifold. We visualize them by using diffeomorphism between Hyperbolic space and Poincaré space as described in Section 3.2.

baselines, indicating that superior expressiveness of embedding enables precise targeting. To further demonstrate the effectiveness of our model on general dataset, we present additional experimental results on public benchmark dataset MovieLens. As represented in Table 2, our model shows the best or second-best performance, demonstrating its generality not overfitted to a certain dataset.

Effects of the number of clusters. To illustrate the effect of the number of clusters on the model performance, we report the prediction accuracy and diversity of our model for different T 's. Table 3 shows that the overall performance improves as the cluster grows, and the best performance is obtained at $T = 5$. After $T = 5$, the prediction accuracy converges while the diversity improves further. Overall, we select the T as five throughout the experiments.

Embedding visualization. Figure 4 shows how Multi Manifold Learning works compared to others. From embedding visualization of MLP model and HNN model, we can verify their positive user pool responding to ads are very small. On the other hand, our proposed method Multi-Manifold Learning shows our model includes many users in a positive pool that is compatible with ads.

The data embedding in a different hyperboloid, originating from centroids of different user groups, have different embedding spaces. Since we set two clusters, the Figure 4 shows results for two manifolds. We can verify each manifold has a different distance in the hyperbolic space, ads that are not relevant to the user are pushed to the edge, while preferred ads appear to move toward the center. It is because the hyperbolic space we constructed is centered by the centroids of the well-clustered user group.

6 CONCLUSION

Traditional targeted advertising systems struggle with data representation capabilities because of the inherent limitation of Euclidean space. To tackle this issue, we present Multi-Manifold Learning, a well-designed technique to learn better representation of users and advertisements. Experimental results show the proposed scheme improves the targeted advertising quality in terms of both accuracy

and diversity. As the future directions, we will develop a Multi-Manifold Learning scheme in terms of diffeomorphism learning. Besides, we will extend our method on real-world large scale online service of LINE messenger platform.

ACKNOWLEDGMENTS

The authors would like to thank Professor Hyunwoo J. Kim and NAVER Clova ML X team for insightful comments and discussion.

REFERENCES

- [1] Khaled Alsabti, Sanjay Ranka, and Vineet Singh. 1997. An efficient k-means clustering algorithm. (1997).
- [2] Benjamin Paul Chamberlain, Stephen R Hardwick, David R Wardrope, Fabon Dzugang, Fabio Daolio, and Saúl Vargas. 2019. Scalable hyperbolic recommender systems. *arXiv preprint arXiv:1902.08648* (2019).
- [3] Ines Chami, Zitao Ying, Christopher Ré, and Jure Leskovec. 2019. Hyperbolic graph convolutional neural networks. In *Advances in Neural Information Processing Systems*. 4869–4880.
- [4] Chih-Ming Chen, Chuan-Ju Wang, Ming-Feng Tsai, and Yi-Hsuan Yang. 2019. Collaborative Similarity Embedding for Recommender Systems. In *The World Wide Web Conference*. 2637–2643.
- [5] Tom DuBois, Jennifer Golbeck, John Kleint, and Aravind Srinivasan. 2009. Improving recommendation accuracy by clustering social networks with trust. *Recommender Systems & the Social Web* 532 (2009), 1–8.
- [6] Peter J Forrester and Manjunath Krishnapur. 2009. Derivation of an eigenvalue probability density function relating to the Poincaré disk. *Journal of Physics A: Mathematical and Theoretical* 42, 38 (2009), 385204.
- [7] Octavian Ganea, Gary Bécigneul, and Thomas Hofmann. 2018. Hyperbolic neural networks. In *Advances in neural information processing systems*. 5345–5355.
- [8] Songjie Gong. 2010. A collaborative filtering recommendation algorithm based on user clustering and item clustering. *JSW* 5, 7 (2010), 745–752.
- [9] Mikhael Gromov. 1987. Hyperbolic groups. In *Essays in group theory*. Springer, 75–263.
- [10] Hanjoo Kim, Minkyu Kim, Dongjoo Seo, Jinwoong Kim, Heungseok Park, Soeun Park, Hyunwoo Jo, KyungHyun Kim, Youngil Yang, Youngkwan Kim, et al. 2018. NSML: Meet the MLaaS platform with a real-world case study. *arXiv preprint arXiv:1810.09957* (2018).
- [11] Dmitri Krioukov, Fragkiskos Papadopoulos, Maksim Kitsak, Amin Vahdat, and Marián Boguná. 2010. Hyperbolic geometry of complex networks. *Physical Review E* 82, 3 (2010), 036106.
- [12] Maximilian Nickel and Douwe Kiela. 2017. Poincaré embeddings for learning hierarchical representations. In *Advances in neural information processing systems*. 6338–6347.
- [13] Adam Paszke, Sam Gross, Francisco Massa, Adam Lerer, James Bradbury, Gregory Chanan, Trevor Killeen, Zeming Lin, Natalia Gimelshein, Luca Antiga, Alban Desmaison, Andreas Kopf, Edward Yang, Zachary DeVito, Martin Raison, Alykhan

- Tejani, Sasank Chilamkurthy, Benoit Steiner, Lu Fang, Junjie Bai, and Soumith Chintala. 2019. PyTorch: An Imperative Style, High-Performance Deep Learning Library. In *Advances in Neural Information Processing Systems 32*, H. Wallach, H. Larochelle, A. Beygelzimer, F. d'Alché-Buc, E. Fox, and R. Garnett (Eds.). Curran Associates, Inc., 8024–8035. <http://papers.neurips.cc/paper/9015-pytorch-an-imperative-style-high-performance-deep-learning-library.pdf>
- [14] J Ben Schafer, Dan Frankowski, Jon Herlocker, and Shilad Sen. 2007. Collaborative filtering recommender systems. In *The adaptive web*. Springer, 291–324.
- [15] Timothy Schmeier, Joseph Chisari, Sam Garrett, and Brett Vintch. 2019. Music recommendations in hyperbolic space: an application of empirical bayes and hierarchical poincaré embeddings. In *Proceedings of the 13th ACM Conference on Recommender Systems*. 437–441.
- [16] Nitish Srivastava, Geoffrey Hinton, Alex Krizhevsky, Ilya Sutskever, and Ruslan Salakhutdinov. 2014. Dropout: a simple way to prevent neural networks from overfitting. *The journal of machine learning research* 15, 1 (2014), 1929–1958.
- [17] Nako Sung, Minkyu Kim, Hyunwoo Jo, Youngil Yang, Jingwoong Kim, Leonard Lausen, Youngkwan Kim, Gayoung Lee, Donghyun Kwak, Jung-Woo Ha, et al. 2017. Nsm1: A machine learning platform that enables you to focus on your models. *arXiv preprint arXiv:1712.05902* (2017).
- [18] Lucas Vinh Tran, Yi Tay, Shuai Zhang, Gao Cong, and Xiaoli Li. 2018. HyperML: A Boosting Metric Learning Approach in Hyperbolic Space for Recommender Systems. *James Caverlee, Xia (Ben) Hu, Mounia Lalmas, and Wei Wang, editors, WSDM 20* (2018), 3–7.
- [19] Lyle H Ungar and Dean P Foster. 1998. Clustering methods for collaborative filtering. In *AAAI workshop on recommendation systems*, Vol. 1. Menlo Park, CA, 114–129.
- [20] Ashish Vaswani, Noam Shazeer, Niki Parmar, Jakob Uszkoreit, Llion Jones, Aidan N Gomez, Łukasz Kaiser, and Illia Polosukhin. 2017. Attention is all you need. In *Advances in neural information processing systems*. 5998–6008.
- [21] Suhan Wang, Jiliang Tang, Yilin Wang, and Huan Liu. 2015. Exploring Implicit Hierarchical Structures for Recommender Systems.. In *IJCAI*. 1813–1819.
- [22] Hong-Jian Xue, Xinyu Dai, Jianbing Zhang, Shujian Huang, and Jiajun Chen. 2017. Deep Matrix Factorization Models for Recommender Systems.. In *IJCAI*. 3203–3209.
- [23] Baolin Yi, Xiaoxuan Shen, Hai Liu, Zhaoli Zhang, Wei Zhang, Sannyuya Liu, and Naixue Xiong. 2019. Deep matrix factorization with implicit feedback embedding for recommendation system. *IEEE Transactions on Industrial Informatics* 15, 8 (2019), 4591–4601.
- [24] Fuzheng Zhang, Nicholas Jing Yuan, Defu Lian, Xing Xie, and Wei-Ying Ma. 2016. Collaborative knowledge base embedding for recommender systems. In *Proceedings of the 22nd ACM SIGKDD international conference on knowledge discovery and data mining*. 353–362.
- [25] Shuai Zhang, Lina Yao, Aixin Sun, and Yi Tay. 2019. Deep learning based recommender system: A survey and new perspectives. *ACM Computing Surveys (CSUR)* 52, 1 (2019), 1–38.
- [26] Yuanxing Zhang, Zhuqi Li, Chengliang Gao, Kaigui Bian, Lingyang Song, Shaoling Dong, and Xiaoming Li. 2018. Mobile social big data: Wechat moments dataset, network applications, and opportunities. *IEEE Network* 32, 3 (2018), 146–153.